Low-lying excited states in the neutron-deficient isotopes ^{163}Os and ^{165}Os

M. C. Drummond,[1] D. T. Joss,[1,*] R. D. Page,[1] J. Simpson,[2] D. O'Donnell,[1] K. Andgren,[3] L. Bianco,[1,†] B. Cederwall,[3] I. G. Darby,[1,‡] S. Eeckhaudt,[4] M. B. Gomez-Hornillos,[2] T. Grahn,[4] P. T. Greenlees,[4] B. Hadinia,[3,§] P. M. Jones,[4] R. Julin,[4] S. Juutinen,[4] S. Ketelhut,[4] A.-P. Leppänen,[4] M. Leino,[4] M. Nyman,[4] J. Pakarinen,[4] P. Rahkila,[4] M. Sandzelius,[3,‖] P. J. Sapple,[1] J. Sarén,[4] B. Saygi,[1] C. Scholey,[4] J. Sorri,[4] J. Thomson,[1] J. Uusitalo,[4] and M. Venhart[5]

[1]*Oliver Lodge Laboratory, University of Liverpool, Liverpool L69 7ZE, United Kingdom*

[2]*STFC, Daresbury Laboratory, Daresbury, Warrington WA4 4AD, United Kingdom*

[3]*Department of Physics, Royal Institute of Technology, S106 91 Stockholm, Sweden*

[4]*Department of Physics, University of Jyväskylä, PO Box 35, FI-40014 Jyväskylä, Finland*

[5]*Institute of Physics, Slovak Academy of Sciences, SK-84511 Bratislava, Slovakia*

(Received 11 March 2013; published 10 May 2013)

Excited states in the neutron-deficient isotopes ^{163}Os and ^{165}Os were identified using the JUROGAM and GREAT spectrometers in conjunction with the RITU gas-filled separator. The ^{163}Os and ^{165}Os nuclei were populated via the ^{106}Cd(^{60}Ni,3n) and ^{92}Mo(^{78}Kr,2p3n) reactions at bombarding energies of 270 MeV and 357 MeV, respectively. Gamma-ray emissions from these nuclei have been established unambiguously using the recoil-decay tagging technique and a coincidence analysis has allowed level schemes to be established. These results suggest that the yrast states are based upon negative-parity configurations originating from the $\nu f_{7/2}$ and $\nu h_{9/2}$ orbitals.

DOI: 10.1103/PhysRevC.87.054309 PACS number(s): 27.70.+q, 23.20.Lv, 29.30.Kv

I. INTRODUCTION

The identification of excited states in atomic nuclei spanning complete shells is crucial to determining the evolution of nuclear structure from both empirical and theoretical perspectives. The osmium isotopes currently represent the best opportunity to probe the evolution of nuclear structure across the $82 \leqslant N \leqslant 126$ neutron shell. The existence of the osmium isotopes in an uninterrupted sequence from ^{161}Os$_{85}$ [1] to ^{203}Os$_{127}$ [2] has been established [2,3], while excited states have been identified in these known nuclei below ^{200}Os$_{124}$ [4] with the exception of the odd-mass isotopes below $N = 89$. The excitation level schemes across the shell reveal the transitions between the single-particle and collective regimes as a function of neutron number.

The low-lying energy spectra in the osmium isotopes have been investigated from different theoretical perspectives. For example, the neutron-deficient osmium isotopes have been discussed in terms of general collective models [5], shape coexistence [6–8], and phase transitions between the limiting symmetries of the interacting boson approximation [9]. However, most theoretical investigations have focused on the even-N isotopes above ^{170}Os$_{94}$ and little is known about the transition to single-particle structures as the $N = 82$ closed shell is approached.

The discovery of yrast states in the Os isotopes at greater neutron deficiency has burgeoned with the advent of selective tagging techniques [10–14]. Prior to this work, γ-ray transitions in ^{165}Os have been identified but no level scheme of excited states was proposed [12]. However, the spin and parity of the ground state of ^{165}Os have been assigned to be $7/2^-$ on the basis of the measured proton and α radioactivity observed in a correlated decay chain originating from ^{170}Au [15]. The ground state of ^{163}Os is also assigned as having spin and parity $7/2^-$ on the basis of the low hindrance factor of its α decay to the $7/2^-$ ground state of ^{159}W [16,17]. This paper reports the first level schemes for ^{163}Os$_{87}$ and ^{165}Os$_{89}$ providing knowledge of low-lying yrast states in an unbroken chain of isotopes from ^{162}Os$_{86}$ [10] to ^{199}Os$_{123}$ [4].

II. EXPERIMENTAL DETAILS

Excited states in ^{163}Os and ^{165}Os were populated using the reactions listed in Table I. The beam species were accelerated by the K130 cyclotron at the University of Jyväskylä Accelerator Laboratory. Gamma rays emitted at the target position were detected by the JUROGAM spectrometer, comprising 43 escape-suppressed HPGe detectors [18]. Fusion-evaporation residues recoiling from the target were separated from scattered beam and transported to the focal plane by the RITU gas-filled separator [19–21]. At the focal plane fusion-evaporation residues were implanted into the double-sided silicon strip detectors (DSSDs) of the GREAT spectrometer [22]. The GREAT multiwire proportional counter provided energy loss and (in conjunction with the DSSDs) time-of-flight information, which allowed the recoils to be distinguished from the scattered beam and subsequent radioactive decays. All detector signals were time stamped and recorded by the total data readout data acquisition system [23], which allowed

*Corresponding author: david.joss@liv.ac.uk

†Present address: DESY, Notkestraße 85, 22607 Hamburg, Germany.

‡Present address: IAEA Nuclear Spectrometry and Applications Laboratory, Physics Section, A-2444 Siebersdorf, Austria.

§Present address: University of Guelph, Department of Physics, Guelph, ON N1G 2W1, Canada.

‖Present address: Department of Physics, University of Jyväskylä, PO Box 35, FI-40014 Jyväskylä, Finland.

TABLE I. Summary of reactions employed in the present work.

Experiment	Beam species	Beam energy (MeV)[a]	Average beam current (pnA)	Target isotope	Thickness (mg/cm^2)	Exit channel	Residual nucleus	Duration of experiment (h)
1	^{60}Ni	270	4	^{106}Cd	1.1	$3n$	^{163}Os	120
2	^{78}Kr	357	6	^{92}Mo	0.5	$3n2p$	^{165}Os	172
3	^{78}Kr	357	6	^{92}Mo	1.0	$3n2p$	^{165}Os	26

[a]Bombarding energy at the front of the target.

implanted nuclei to be identified through temporal and spatial correlations with their subsequent radioactive decays. These data were sorted offline and analyzed using the GRAIN [24] and ESCL8R [25] software analysis packages.

III. RESULTS

A. ^{163}Os ($N = 87$)

The recoil-decay tagging (RDT) technique correlates γ rays emitted promptly at the target position with the characteristic radioactive decays of the residual nucleus at the focal plane of a recoil separator [26–28]. The RDT technique provides high-confidence correlations under the optimum conditions of short decay half-lives and high decay branching ratios. The α-emitting nucleus ^{163}Os has decay properties well suited to RDT spectroscopy. The half-life of ^{163}Os has been measured to be 5.5 ± 0.6 ms with an α-decay branching ratio close to 100% [16]. A total of 10 656 full-energy ($E_\alpha = 6510$ keV) α(^{163}Os) decays was observed in Experiment 1 (see Table I). Assuming a RITU separation efficiency of 50% [21] and an efficiency of 65% for full-energy α-particle detection, this yield corresponds to a cross section of $\sim$0.5 μb. Figure 1(a) shows γ rays correlated with recoil implantations followed by the characteristic α decay of ^{163}Os within the same DSSD pixel of the GREAT spectrometer. The recoil-decay correlation time was limited to 25 ms. The measured properties of γ rays in ^{163}Os are listed in Table II.

A significant fraction of α particles escape from the DSSD without depositing their full energy. However, it is possible to utilize these decays if there is a distinct daughter α decay with appropriate decay properties. Figure 1(b) shows a γ-ray spectrum obtained by demanding correlations with escaping α particles that are followed by the distinct daughter α decay of ^{159}W [29] within the same DSSD pixel. The $E_\alpha = 6292$ keV decay line in ^{159}W has been measured previously to have a high α-decay branching ratio (92%) and a half-life of 8.2 ± 0.7 ms [29], which is sufficiently short to give clean correlations with escaping ^{163}Os α particles. In these data 2822 escaping α decays satisfied the criteria and were added to the statistics for the γ-ray coincidence analysis. Figure 1(b) shows that the γ-ray counting statistics may be augmented through escape correlations without increasing the γ-ray background noticeably. Even so, a meaningful angular correlation analysis was not possible with these data due to the low level of statistics, which precluded unambiguous multipolarity assignments for the measured γ rays.

A recoil-decay tagged $\gamma\gamma$-coincidence matrix correlated with the full-energy and escape α(^{163}Os) particles was produced from these data. This matrix demonstrated that the 238, 624, 669, and 700 keV γ rays are in coincidence forming a cascade. Figure 1(c) shows a summed coincidence spectrum for these transitions. This cascade is assumed to be composed

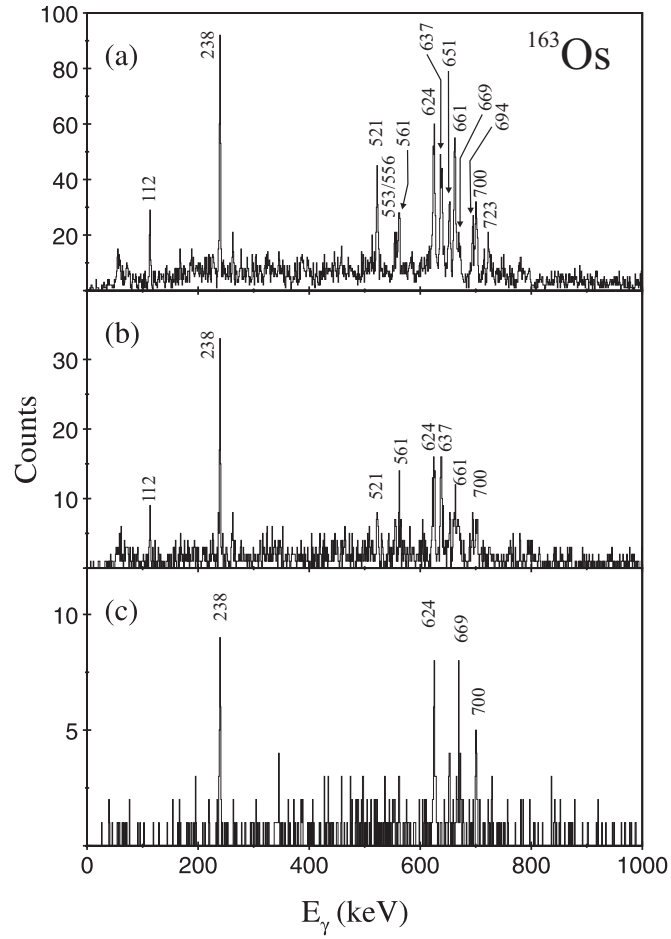

FIG. 1. (a) Gamma rays correlated with recoil implantations followed by the characteristic α decay of ^{163}Os within the same DSSD pixel of the GREAT spectrometer. (b) Gamma rays correlated with escaping α(^{163}Os) followed by the daughter α(^{159}W) decay within the same pixel of the DSSD. The energy range for the escape α particle was limited to 500–4000 keV. The correlation time was limited to 25 ms for the first decay and 32 ms for the second decay. (c) Gamma rays in coincidence with the 624, 669, 700, or 238 keV transitions generated from a $\gamma\gamma$-coincidence matrix correlated with ^{163}Os full-energy and escape α correlations.

TABLE II. Transition energies and relative intensities of γ rays assigned to ^{163}Os and ^{165}Os obtained from the pertinent α-correlated γ-ray singles spectrum. The error on the transition energies ranges from ≈ 0.5 keV to 1 keV. The angular intensity ratios R_θ for ^{165}Os are listed (see text for details).

^{163}Os		^{165}Os		
E_γ (keV)	I_γ (%)	E_γ (keV)	I_γ (%)	R_θ
112.0	23(3)	95.2	14(3)	0.6(3)
238.4	42(4)	384.3	13(2)	
521.4	31(4)	388.7	10(2)	
553.1	9(3)	489.6	79(3)	0.9(1)
556.0	6(3)	499.3	100(3)	1.1(1)
561.0	20(4)	518.0	33(3)	
623.7	100(7)	539.8	13(3)	
636.9	65(7)	558.6	38(3)	1.3(4)
651.4	26(6)	584.9	25(4)	
661.3	73(6)	593.0	19(4)	
668.5	39(4)	596.7	97(5)	0.9(2)
693.6	14(3)	604.5	16(2)	
700.0	43(5)	633.2	64(4)	0.9(2)
722.5	27(3)	656.1	24(3)	0.9(3)
		691.6	15(2)	
		699.8	43(3)	

of stretched $E2$ transitions feeding the ground state. The 624 keV peak is the most intense γ ray and is assumed to be the $(11/2^-) \rightarrow 7/2^-$ transition. The ordering of the 669, 700, and 238 keV transitions could not be unambiguously established from the intensity measurements and coincidence relationships, so the ordering is based on the systematics of excited states in the light Os nuclei. The excitation energy of the $(23/2^-)$ state is insensitive to the ordering of these γ rays. The 651 keV transition is observed to be in coincidence only with the 624 keV transition and is assigned to feed the $(11/2^-)$ state. The level scheme deduced for ^{163}Os is presented in Fig. 2.

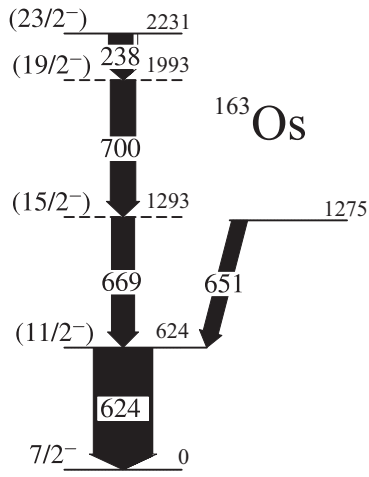

FIG. 2. Level scheme deduced for ^{163}Os. The transition energies are in keV and their relative intensities are proportional to the width of the arrows. The white arrow components reflect the estimated internal conversion intensity.

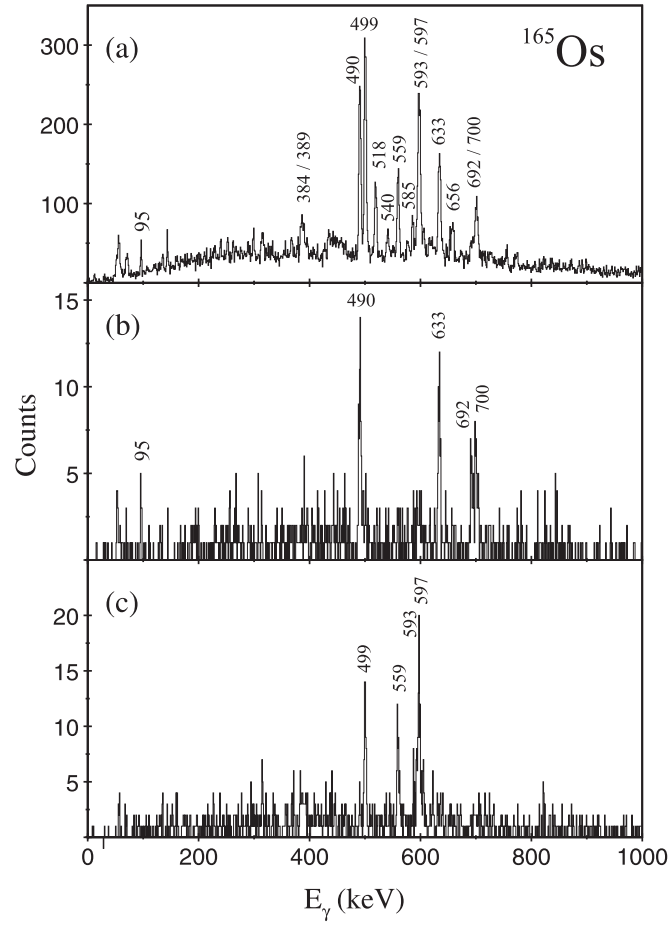

FIG. 3. (a) Gamma rays correlated with recoil implantations followed by the characteristic α decay of ^{165}Os within the same DSSD pixel of the GREAT spectrometer. (b) Summed γ-ray spectrum in coincidence with the 490, 633, 700, or 692 keV transitions generated from an $\alpha(^{165}\text{Os})$-correlated $\gamma\gamma$-coincidence matrix. (c) Summed γ-ray spectrum in coincidence with the 499, 597, 559, or 593 keV transitions generated from an $\alpha(^{165}\text{Os})$-correlated $\gamma\gamma$-coincidence matrix. The recoil-α correlation time was limited to 280 ms in each case.

The relatively strong 661, 637, and 521 keV transitions that are associated with ^{163}Os, see Fig. 1(a) and Table II, do not appear to be in prompt coincidence with the main cascade and could not be placed in the level scheme.

B. ^{165}Os ($N = 89$)

The neutron-deficient nucleus ^{165}Os is an α-emitting nucleus with decay properties that are also ideally suited for recoil-decay tagging. The half-life of ^{165}Os has been measured to be 72 ± 3 ms with a branching ratio close to 100% [29]. A total of 149 953 full-energy ($E_\alpha = 6188$ keV) $\alpha(^{165}\text{Os})$ decays was observed in Experiments 2 and 3 (see Table I), corresponding to a cross section of ~ 5 μb, assuming a RITU separation efficiency of 50% [21] and an efficiency of 65% for full-energy α-particle detection. Figure 3(a) shows γ rays correlated with recoil implantations followed by the characteristic α decay of ^{165}Os within the same DSSD pixel

of the GREAT spectrometer. The recoil-decay correlation time was limited to 280 ms. The measured properties of γ rays in ^{165}Os are listed in Table II.

The γ-ray spectrum in Fig. 3(a) shows the same transitions discovered by Appelbe *et al.* in an earlier RDT experiment probing ^{165}Os [12]. In that experiment there were insufficient coincidence data to determine an excitation level scheme. Given the complex character of the spectra in nuclei approaching the single-particle regime, γ-ray coincidence analyses are crucial for ordering the excitation level schemes. Figures 3(b) and 3(c) show summed γ-ray coincidences obtained from an $\alpha(^{165}\text{Os})$-correlated $\gamma\gamma$-coincidence matrix. Correlations with the escaping $\alpha(^{165}\text{Os})$ decays were not included due to the γ-ray background generated by correlations with the daughter, ^{161}W ($t_{1/2} = 409 \pm 18$ ms, $b_\alpha = 73 \pm 3\%$) [29], which is significantly longer lived than the ^{163}Os daughter, ^{159}W. Multipolarity assignments for the strongest γ-ray transitions in ^{165}Os were obtained from angular intensity ratios, R_θ. In this method a ratio of $\alpha(^{165}\text{Os})$-correlated γ-ray intensities detected at the $\theta = (158^\circ$ and $134^\circ)$ and $\theta = (94^\circ$ and $86^\circ)$ spectrometer angles was extracted. The method employed discriminated between different multipolarities in ^{166}W yielding typical R_θ values of approximately 1 and 0.6 for stretched quadrupole and stretched dipole transitions, respectively [30]. The angular intensity ratios extracted for ^{165}Os are listed in Table II. Figure 4 shows the level scheme deduced on the basis of γ-ray coincidences, relative intensities and angular intensity ratios.

While the level of counts is very low, these summed coincidence spectra suggest that there are two distinct low-spin structures in ^{165}Os. Figure 3(b) shows γ rays in coincidence with the 490, 633, 700, or 692 keV γ rays, which form the left-hand side of Fig. 4. It is assumed that the 95 keV transition, which is not apparent in Fig. 3(c), is a stretched magnetic dipole transition connecting a stretched $E2$ cascade to the $7/2^-$ ground state as observed in $^{167}\text{Os}_{87}$ [13]. Allowing for the total conversion coefficient of 6.5 for a 95 keV $M1$ transition [31], the intensity of this transition is greater than that of the 490 keV $E2$ transition feeding the $9/2^-$ state. A parallel sequence of γ rays comprising the 499, 597, 559, and 593 keV transitions (shown on the right-hand side of Fig. 4) is also assumed to feed the ground state based on comparisons with the structure of ^{167}Os [13]. The energy spectrum of these summed γ-ray coincidences is shown in Fig. 3(c).

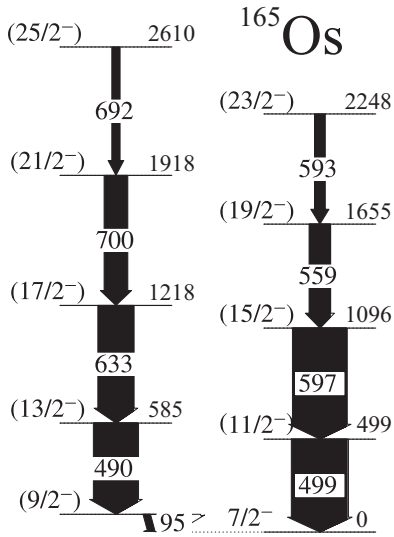

FIG. 4. Level scheme deduced for ^{165}Os. The transition energies are in keV and their relative intensities are proportional to the width of the arrows. The white arrow components reflect the estimated internal conversion intensity.

IV. DISCUSSION

The low-lying states in the neutron-deficient osmium isotopes are based on single quasiparticle configurations formed when the odd neutron occupies one of the available $f_{7/2}$, $h_{9/2}$, or $i_{13/2}$ states near the Fermi surface [32–36]. Figure 5 compares selected low-lying excited states in ^{163}Os and ^{165}Os with the ground-state bands in their lighter even-N neighbors. The low-lying states in ^{163}Os and ^{165}Os fit in with the systematic trend of the light Os isotopes of increasing excitation energy in nuclei closer to $N = 82$. This indicates a change in structure from collective rotations in the $N > 90$ Os isotopes towards a single-particle regime. Indeed, in ^{162}Os a low-lying 8^+ state was identified and interpreted as the $(f_{7/2}, h_{9/2})_{8^+}$ or $(h_{9/2})^2_{8^+}$ configuration [10]. The low-lying $23/2^-$ state in ^{163}Os lies between the 8^+ states in the neighboring even-N isotopes. Therefore, the $23/2^-$ states is interpreted as the maximally aligned $(f_{7/2}, h^2_{9/2})_{23/2^-}$ state.

There is evidence in this mass region for the existence of a low-lying $13/2^+$ isomer based on a configuration where the odd neutron occupies the $i_{13/2}$ orbital. The relative ordering of the single-quasiparticle excitations in nearby nuclei has been deduced from the electromagnetic decay paths of the $13/2^+$ isomeric state. For example, Scholey *et al.* measured the half-lives of the $13/2^+$ isomers in ^{163}W and ^{167}Os to be 154 ± 3 ns and 672 ± 7 ns, respectively, and deduced that the decay path comprises an $M2$ transition to the $9/2^-$ state followed by an $M1$ transition to the $7/2^-$ ground state, see Fig. 6. Thus, the first excited structure is interpreted as a single quasineutron

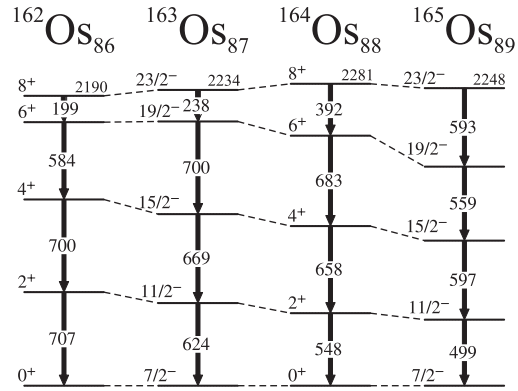

FIG. 5. Comparison of energy levels in ^{163}Os and ^{165}Os with the ground state bands in their lighter even-N neighbors. All levels are placed relative to the ground state. All level spin assignments are tentative. The dashed lines connect states with similar structure.

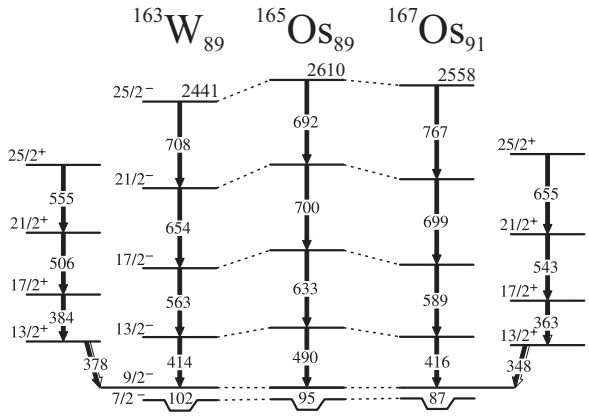

FIG. 6. Comparison of energy levels in ^{165}Os with its heavier odd-N isotope ^{167}Os and its lower-Z isotone ^{163}W. All levels are placed relative to the ground state. All level spin assignments are tentative. The dashed lines connect states with similar structure.

configuration based upon the $h_{9/2}$ orbital. Figure 6 compares the excited states based upon the $(9/2^-)$ state in ^{165}Os with the structures based on the $h_{9/2}$ configuration in the lighter even-Z ($N = 89$) isotone ^{163}W [37] and the heavier odd-N isotope ^{167}Os [13]. This structure in ^{165}Os shows a marked similarity with these neighboring nuclei and is also assumed to be based on the $h_{9/2}$ state. The $\nu i_{13/2}$ band built on the $13/2^+$ isomer is the most intense structure in the yrast spectra of nearby odd-N nuclei, such as the $\nu i_{13/2}$ bands in ^{163}W and ^{167}Os shown in Fig. 6. However, in ^{165}Os only excited states built upon the $\nu f_{7/2}$ and $\nu h_{9/2}$ configurations have been observed. The absence of this structure in ^{165}Os is consistent with the trend of increasing excitation energy of the $i_{13/2}$ state with decreasing neutron number in the Os [13,32], W [37,38], and Ta [39] isotopes when approaching the $N = 82$ shell closure.

V. CONCLUSIONS

Gamma-ray transitions have been observed for the first time in the highly neutron-deficient nucleus ^{163}Os. The low-lying yrast structure has been established to a tentative spin and parity $23/2^-$ corresponding to the maximally aligned $(f_{7/2}, h^2_{9/2})_{23/2^-}$ state. A level scheme for the heavier odd-N isotope ^{165}Os has also been established for the first time. The level structures in both nuclei are interpreted in terms of configurations involving the negative-parity $f_{7/2}$ and $h_{9/2}$ neutron orbitals and reflect the transition from γ-soft shapes observed in the heavier isotopes to near-spherical shapes near the closed $N = 82$ shell. The observation of excited states in ^{163}Os and ^{165}Os completes the knowledge of excited states in the osmium nuclides spanning an uninterrupted isotopic chain from ^{162}Os$_{86}$ to ^{199}Os$_{123}$.

ACKNOWLEDGMENTS

Financial support for this work has been provided by the UK Science and Technology Facilities Council, the EU 6th Framework Programme, "Integrating Infrastructure Initiative - Transnational Access", contract no. 506065 (EURONS), the Academy of Finland under the Finnish Centre of Excellence Programme (Nuclear and Accelerator-based Physics Programme at JYFL), Slovak grant agency VEGA (contract no. 2/0105/11), the Slovak Research and Development Agency (contract no. APVV-0177-11), and the Swedish Research Council. T.G., P.T.G., and C.S. acknowledge the support of the Academy of Finland. The authors express their gratitude to the staff of the Accelerator Laboratory at the University of Jyväskylä for their excellent technical support. The authors also wish to thank Paul Morrall of the STFC Daresbury Laboratory for the preparation of the targets used in this work.

[1] L. Bianco *et al.*, Phys. Lett. B **690**, 15 (2010).
[2] J. Kurcewicz *et al.*, Phys. Lett. B **717**, 371 (2012).
[3] R. Robinson and M. Thoennessen, At. Data Nucl. Data Tables **98**, 911 (2012).
[4] S. J. Steer *et al.*, Phys. Rev. C **84**, 044313 (2011).
[5] L. Fortunato, S. DeBaerdemacker, and K. Heyde, Phys. Rev. C **74**, 014310 (2006).
[6] T. Kibedi, G. D. Dracoulis, A. P. Byrne, P. M. Davidson, and S. Kuyucak, Nucl. Phys. A **567**, 183 (1994).
[7] P. M. Davidson, G. D. Dracoulis, T. Kibedi, A. P. Byrne, S. S. Anderssen, A. M. Baxter, B. Fabricius, G. J. Lane, and A. E. Stuchbery, Nucl. Phys. A **568**, 90 (2001).
[8] J. L. Wood and K. Heyde, Rev. Mod. Phys. **83**, 1467 (2011).
[9] E. A. McCutchan and N. V. Zamfir, Phys. Rev. C **71**, 054306 (2005).
[10] D. T. Joss *et al.*, Phys. Rev. C **70**, 017302 (2004).
[11] S. L. King *et al.*, Phys. Rev. C **62**, 067301 (2000).
[12] D. E. Appelbe *et al.*, Phys. Rev. C **66**, 014309 (2002).
[13] D. O'Donnell *et al.*, Phys. Rev. C **79**, 064309 (2009).
[14] D. T. Joss *et al.*, Nucl. Phys. A **689**, 631 (2001).
[15] H. Kettunen *et al.*, Phys. Rev. C **69**, 054323 (2004).
[16] C. R. Bingham *et al.*, Phys. Rev. C **54**, R20 (1996).
[17] P. J. Sapple *et al.*, Phys. Rev. C **84**, 054303 (2011).
[18] C. W. Beausang *et al.*, Nucl. Instrum. Methods Phys. Res. A **313**, 37 (1992).
[19] M. Leino *et al.*, Nucl. Instrum. Methods Phys. Res. B **126**, 320 (1997).
[20] J. Uusitalo *et al.*, Nucl. Instrum. Methods Phys. Res. B **204**, 638 (2003).
[21] J. Sarén, J. Uusitalo, M. Leino, and J. Sorri, Nucl. Instrum. Methods Phys. Res. A **654**, 508 (2011).
[22] R. D. Page *et al.*, Nucl. Instrum. Methods Phys. Res. B **204**, 634 (2003).
[23] I. H. Lazarus *et al.*, IEEE Trans. Nucl. Sci. **48**, 567 (2001).
[24] P. Rahkila, Nucl. Instrum. Methods Phys. Res. A **595**, 637 (2008).
[25] D. C. Radford, Nucl. Instrum. Methods Phys. Res. A **361**, 297 (1995).
[26] K.-H. Schmidt, R. S. Simon, J.-G. Keller, F. P. Hessberger, G. Münzenberg, B. Quint, H.-G. Clerc, W. Schwab, U. Gollerthan, and C.-C. Sahm, Phys. Lett. B **168**, 39 (1986).
[27] R. S. Simon, K.-H. Schmidt, F. P. Hessberger, S. Hlavac, M. Honusek, G. Münzenberg, H.-G. Clerc, U. Gollerthan, and W. Schwab, Z. Phys. A **325**, 197 (1986).
[28] E. S. Paul *et al.*, Phys. Rev. C **51**, 78 (1995).

[29] R. D. Page, P. J. Woods, R. A. Cunningham, T. Davinson, N. J. Davis, A. N. James, K. Livingston, P. J. Sellin, and A. C. Shotter, Phys. Rev. C **53**, 660 (1996).
[30] J. Simpson, F. Hanna, M. A. Riley, A. Alderson, M. A. Bentley, A. M. Bruce, D. M. Cullen, P. Fallon, and L. Walker, J. Phys. G **18**, 1207 (1992).
[31] T. Kibédi, T. W. Burrows, M. B. Trzhaskovskaya, P. M. Davidson, and C. W. Nestor Jr., Nucl. Instrum. Methods Phys. Res. A **589**, 202 (2008).
[32] R. A. Bark *et al.*, Nucl. Phys. A **646**, 399 (1999).
[33] R. A. Bark, G. D. Dracoulis, and A. E. Stuchbery, Nucl. Phys. A **514**, 503 (1990).
[34] C. A. Kalfas *et al.*, Nucl. Phys. A **526**, 205 (1991).
[35] B. Fabricius, G. D. Dracoulis, R. A. Bark, A. E. Stuchbery, T. Kibedi, and A. M. Baxter, Nucl. Phys. A **511**, 345 (1990).
[36] G. D. Dracoulis, C. Fahlander, and A. P. Byrne, Nucl. Phys. A **401**, 490 (1983).
[37] J. Thomson *et al.*, Phys. Rev. C **81**, 014307 (2010).
[38] G. D. Dracoulis *et al.*, Proceedings of the International Conference on Nuclear Structure High Angular Momentum, Ottawa, AECL Report No. 10613 **2**, 94 (1992).
[39] K. Lagergren *et al.*, Phys. Rev. C **83**, 014313 (2011).